Behaviour and Design of a Self-Centering Concentrically Braced Steel Frame System

G.J. O'Reilly, J. Goggins
National University of Ireland, Galway.

S.A. Mahin
University of California, Berkeley.

SUMMARY
Concentrically braced frames (CBFs) are designed to undergo numerous cycles of inelastic deformation through the tensile yielding and inelastic global buckling of its bracing members. This inelastic behaviour leads to the possibility that structures designed according to current codified approaches are likely to have residual deformations after a major seismic event. This paper presents a new type of self-centering system that uses tubular brace members together with a post-tensioning arrangement to give a self-centering concentrically braced frame (SC-CBF). A numerical model of this SC-CBF is developed and a design example of a 3-storey frame is presented to demonstrate the performance of the SC-CBF against some performance goals. The results from a series of time-history analyses show that the SC-CBF is a system capable of withstanding large seismic forces, while also minimising residual drifts following a major seismic event.

Keywords: self-centering, residual drift, concentrically braced frames, steel.

1. INTRODUCTION

Structures which are designed for the design basis earthquake (DBE) are expected to exhibit many cycles of inelastic deformation to dissipate hysteretic energy during seismic loading. For a concentrically braced frame (CBF), these inelastic deformations are through the tensile yielding and inelastic buckling of what are most often tubular steel bracing members. Hence, this inelastic behaviour of the system leads to the large possibility of residual deformations being present in the structure after the DBE, even if the system has performed exactly as intended. These residual deformations, or drifts, can be extremely problematic given the difficulties associated with attempting to straighten a structure following a seismic event. An investigation into the effects of residual drifts in Japan (McCormick *et al.* 2008) concluded that once the residual drifts in a structure exceed 0.5%, the occupants of the building begin to experience nausea, headaches and an overall hindrance on daily life. It was concluded during this study that for 12 case study steel-framed buildings following the Hyogoken-Nanbu earthquake in 1995, where the residual interstorey drifts exceeded 0.5%, it was more financially viable to demolish and rebuild the structure rather than attempt to repair it due to the repair costs and economical losses that would be incurred with the building closed during the repair period. While attempts have been made to incorporate the occurrence of residual drifts in structures into the design procedure to ensure excessive residual drifts do not occur, the use of self-centering systems is becoming more popular.

Extensive research conducted during a joint research initiative called PRESSS in the early 1990's resulted in the conception of the use of post-tensioning as a method of self-centering structural systems. This was done by combining a post-tensioning (PT) system with a energy dissipating system which results in the so-called 'flag shaped' hysteresis loop. This was initially developed for concrete frame and wall systems during the PRESSS project, but has been more recently applied to steel systems, such as moment-resisting frames (MRFs) (Garlock, 2002; Christopoulos, 2002) and steel plate shear wall systems (Clayton *et al*, 2012). The focus of this paper is to introduce a newly

developed self-centering concentrically braced frame (SC-CBF) system, followed by the discussion of a numerical model of the system subjected to cyclic loading. A performance-based design methodology of a 3-storey building using this system is presented. The performance of the system and design methodology is validated through a series of nonlinear time history analyses (NLTHs).

2. SELF-CENTERING SYSTEMS

2.1. Introduction

Since the development of the PRESSS project, numerous different systems have been developed that use a similar self-centering mechanism. These are based around the use of post-tensioning (PT) elements across a gap opening joint that opens and closes during seismic loading. The PT elements remain elastic and their function is solely to force closed the gap opening in the structure, while the energy dissipating system will still exhibit inelastic deformation, but will not result in global residual drifts of the structure. For steel systems, the most common method of self-centering is to use the rocking beam-column connection and the use of a replaceable energy dissipating fuse gives the desired behaviour by recentering the system and localising the damage to replaceable fuse elements.

2.2. Self-Centering Concentrically Braced Frame (SC-CBF)

The purpose of this paper is to present a new system for CBFs that utilises similar technology as previously mentioned systems to give the SC-CBF. Fig. 2.1 shows a general arrangement of the SC-CBF which consists of a 2-bay CBF and a PT element running along the beams and anchored at the exterior columns. The force-displacement hysteretic behaviour of the system is shown in Fig. 2.2, where it can be seen that the combination of the brace deformation and rocking connection gives the desired flag-shaped loop. The achievement of this flag-shaped loop strongly depends on the buckling resistance of the braces, where if more slender braces are used, the compressive resistance is low and the system can be considered almost tension-only bracing. More stockier braces may be used, which is generally a requirement by some design codes, and the flag-shaped loop may still be achieved. However, larger post-tensioning force is required to ensure point 5 in Fig. 2.2 is above zero.

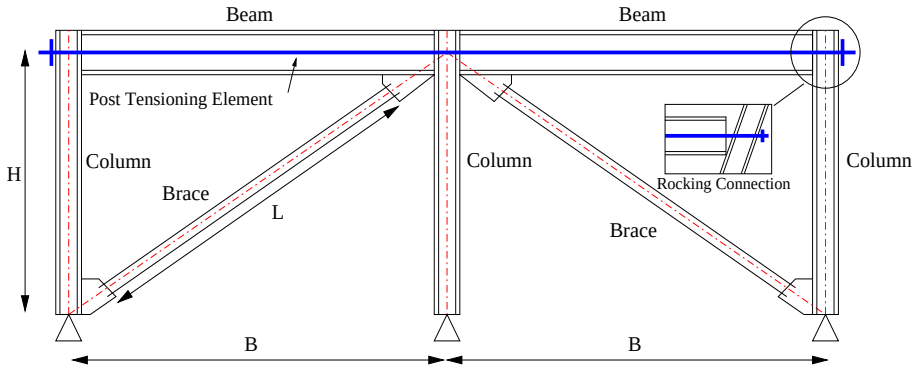

Figure 2.1. General arrangement of a SC-CBF.

Another key feature of the SC-CBF is the connection details of the gusset plates, where typical gusset plates which are welded to both beam and column cannot be used. A beam-only gusset plate is used in order to allow the free rocking behaviour of the beam-column connection, whereas a traditional gusset plate would restrict this gap opening behaviour. Ongoing experimental testing and numerical modelling of these gussets are being conducted at NUI Galway (English & Goggins, 2012), so the design and detailing is not discussed here. The use of large bay widths to frame height ratios will naturally result in the these types of gusset plates, and in addition to this, wider bays result in more slender braces and hence reduce the compression capacity of the brace, which has already been noted as being advantageous.

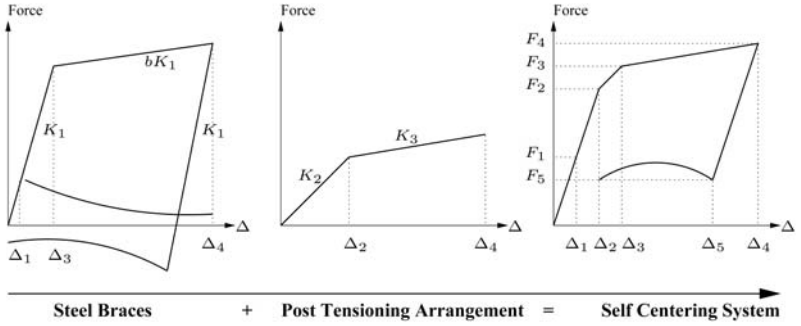

Figure 2.2. Combination of hysteresis rules for the SC-CBF.

2.3. SC-CBF Hysteretic Behaviour

This section discusses the behaviour of the frame shown in Fig. 2.1 and the relationships which give rise to the force-displacement hysteresis shown in Fig. 2.2. As previously mentioned, this system consists of a combination of a rocking connection and a CBF. These behaviours are derived individually and added together to give the desired response.

2.3.1. Brace Response

For a CBF similar to that in Fig. 2.1, but without any PT elements, expressions for K_1, the initial (elastic) lateral frame stiffness, and Δ_3, the lateral yield displacement of the frame due to yielding of the brace member, can be given by Equations 2.1 and 2.2, respectively.

$$K_1 = \frac{A_{br} E B^2}{L^3} \tag{2.1}$$

$$\Delta_3 = \frac{f_y L^2}{BE} \tag{2.2}$$

where A_{br} is the cross-sectional area of the brace, E is the Young's Modulus, B is the bay width, L is the length of the brace and f_y is the yield stress of the bracing member. The contribution of the compressive brace during loading strongly depends on the slenderness of the brace. For slender members, the initial buckling load of the brace may be determined using Euler buckling theory, however the compressive may be determined as per EC3 (CEN, 2005) and this was the approach adopted here .It has been shown that the ultimate resistance of the frame occurs after buckling of the compression brace member has occurred (Broderick *et al*, 2008). Furthermore, during seismic loading, where many cycles of inelastic deformation have occurred, the compressive resistance is significantly reduced in later cycles of inelastic deformation, even at the same displacement demand (Goggins *et al*, 2005). Broderick *et al* (2008) recommended that for braces with normalised slenderness $\bar{\lambda}$ (CEN, 2005) between 1.5 and 2.4, the ultimate resistance of the frame can be estimated from the maximum tensile strength of the tension brace plus 30% of the compression brace buckling capacity, in line with Eurocode 8 provisions (CEN, 2004) for the design of beams in frames with V-bracings. Only for very slender brace members ($\bar{\lambda}$ > 2.4) should the post-buckling resistance of the compression brace be ignored.

2.3.2. Rocking Frame Response

Prior to decompression, the SC-CBF without any bracing members will behave as a moment frame, so the initial stiffness K_2 can be determined using the principle of virtual work. For the frame in Fig. 2.1:

$$K_2 = \left[\frac{H^3}{8EI_c} + \frac{H^2 B}{24EI_b} \right]^{-1} \tag{2.3}$$

where H is the height of the frame and I_c and I_b are the second moment of area of the column and beams respectively. The corresponding displacement at which the response of the frame changes to post-decompression stiffness depends on the level of post-tensioning applied to the frame and the depth of the beam. The compressing moment given by an initial post-tensioning force P_{T0} on a beam with height b_h is given by:

$$M_C = P_{T0} b_h / 2 \tag{2.4}$$

Assuming that the four connections will develop similar moments simultaneously at decompression, the following expression is valid:

$$4M_C = K_2 \Delta_2 H \tag{2.5}$$

where Δ_2 is the roof lateral displacement at which decompression occurs. Equation 2.5 can then be rearranged to give:

$$\Delta_2 = \frac{2P_{T0} b_h}{K_2 H} \tag{2.6}$$

Following decompression, the stiffness of the frame depends on the forces generated in the post-tensioning elements as the gap opening at the rocking at the connection results in an increase in the post-tensioning force, P_T. Christopoulos (2002) derived an expression for the increase in PT forces due to the gap opening and expansion of the frame. Using this derivation, the increase in PT force as function of rotation at the connection θ can be expressed as:

$$P_T = P_{T0} + 2K_{PT}(1 - 1/\Omega) b_h \theta \tag{2.7}$$

where Ω is:

$$\Omega = 1 + \frac{K_b}{K_C + 2K_{PT}} \tag{2.8}$$

where K_b, K_c and K_{PT} are the stiffness of the beam, column and post-tensioning elements, respectively. Equation 2.8 can then be arranged to give an expression for the post decompression lateral frame stiffness K_3 as follows:

$$K_3 = 4K_{PT}\left(1 - \frac{1}{\Omega}\right)\frac{b_h^2}{H^2} \tag{2.9}$$

3. NUMERICAL MODELLING OF SC-CBF

3.1. Model Description

A numerical model that captures the behaviour of the SC-CBF using OpenSees (McKenna *et al.*, 2000) has been developed. The modelling of CBFs in OpenSees has been discussed and developed by

many researchers with the main focus of the research being on accurately capturing the brace behaviour and in particular the development of an appropriate fatigue model for structural hollow steel brace members (for example, Uriz and Mahin, 2008; Wijesundara, 2009; Salawdeh, 2012). These models have been validated against numerous experimental studies. Salawdeh (2012) used a more extensive range of experimental studies, including pseudo-static member tests and full scale shake table frame tests, to validate his module. Hence, the modelling parameters proposed by Salawdeh (2012) are used herein for the SC-CBF.

The rocking frame is a newer concept in steel systems and has been used for various self-centering systems (Garlock, 2002; Christopoulos, 2002; Clayton *et al.* 2012). The modelling approach that has been used by many researchers is to employ a series of contact springs and rigid links to represent the rocking of the beam against the column during cyclic loading. Fig. 3.1 shows the basic arrangement, where the rigid links are used to represent the face of the column and also the face of the top and bottom flanges of the beam. Using as series of contact springs, the rocking of the connection can be modelled. Fig. 3.1 shows the complete model used for the SC-CBF, where the bracing members are connected to the beams, as for a beam-only gussets and these beams, columns and braces are modelled using a fibre element based on the force based formulation. This modelling procedure has been verified against existing experimental data by Garlock (2002) and Christopoulos (2002), where the post-tensioned rocking connection was tested under cyclic loading. Using the modelling procedure discussed here for the rocking connection, these experimental results were closely replicated numerical, therefore validating the proposed approach to modelling the rocking connection.

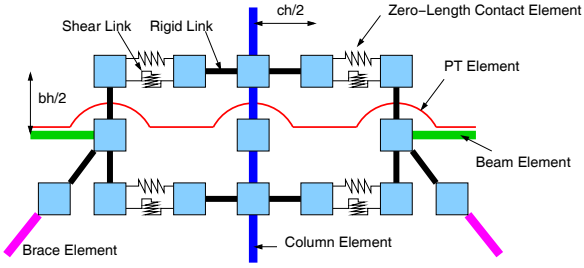

Figure 3.1. SC-CBF rocking connection model arrangement.

3.2. Quasi-Static Loading

To demonstrate the flag-shaped behaviour of the SC-CBF and the response of an example 1-storey, 2-bay frame as shown in Figure 2.1 is presented and plotted along with the expressions derived in Eqns. 2.1 – 2.9. The frame consists of *HE320A* columns, *IPE600* beams and *100x100x8SHS Grade S275* braces. The PT elements consist of 2 no. 30*mm* diameter cables with a 500*kN* pre-stress applied to them, which are then anchored at the two exterior nodes. This frame is then cycled through 0.5, 1.0, 2.0, 3.0 and 4.0 % drift cycles. The resulting plot of base shear versus interstorey drift is shown in Fig. 3.2. It can be seen that the system exhibits the flag shaped hysteresis required to achieve self-centering, and furthermore that the simplified expressions developed in Eqns. 2.1 – 2.9 capture the behaviour with reasonable accuracy.

4. DESIGN OF A 3-STOREY SC-CBF

4.1. Force-Based Design Procedure

The following section describes the design of a 3-storey SC-CBF according to the force-based design procedure set out in Eurocode 8 (EC8) (CEN, 2004). The expressions derived in Section 2 are used to estimate the storey resisting forces in the SC-CBF and hence design the frame accordingly. Fig. 4.1 shows the layout of the building under consideration, which consists of four individual SC-CBFs with two of these in each direction. The building being designed is situated in downtown Los Angeles, and

the design basis earthquake (DBE) is taken as the 10% probability of exceedence in 50 year event. The corresponding design spectrum being used here corresponds to the spectral values set out in Somerville *et al.* (1997), as given in Figure 4.2. Note also that this is the spectrum the ground motions described later are scaled to match.

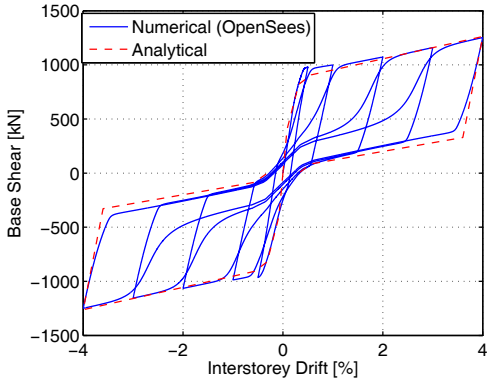

Figure 3.2. Base shear versus interstorey drift of a 1-storey SC-CBF.

A behaviour factor (q) of 4 has been adopted here as per EC8, and using the first mode period, which can be initially obtained using the codes height based formula, or from an eigenvalue analysis of the OpenSees model during subsequent iterations, the base shear is obtained. This is then distributed along the height of the building as per the Equivalent Lateral Force method described in the code. The storey resisting shear force (V_i) is then determined using the expressions previously derived as:

$$V_i = (K_1 + K_2)\Delta_2 + (K_1 + K_3)(\Delta_3 - \Delta_2) \tag{4.1}$$

The interstorey drift of the frame was limited to 2.5%, which is commonly specified in many codes in the force-based design procedure. The beams and column forces were obtained from a pushover analyses and these were capacity designed to ensure elastic behaviour. The beams and columns were then conservatively designed as follows:

$$\frac{N_{ED}}{N_{RD}} + \frac{M_{ED}}{M_{RD}} \leq 1 \tag{4.2}$$

which accounts for the axial moment interaction of the members. The PT elements were designed to an interstorey drift of 2.5% using Eqn. 2.7 and P-Delta effects were checked using the inequality:

$$4K_3 - mg > 0 \tag{4.3}$$

The resulting design of the 3-storey SC-CBF is given in Table 4.1, where the beams, columns and braces were designed with grade S355 steel having a Young's modulus of 210*GPa*, whereas the PT elements were designed with a yield stress of 1650*MPa* and modulus of 210*GPa*. The PT strands were 10mm in diameter. An eigenvalue analysis gave the first fundamental period to be 0.51s.

Table 4.1. Prototype 3-storey SC-CBF design.

Storey	Braces	Columns	Beams	PT Force [kN]	No. of Strands
3	80x80x8-SHS	HE240M	IPE400O	179	6
2	100x100x10-SHS	HE300M	IPE450V	511	8
1	100x100x12-SHS	HE400M	IPE600V	775	10

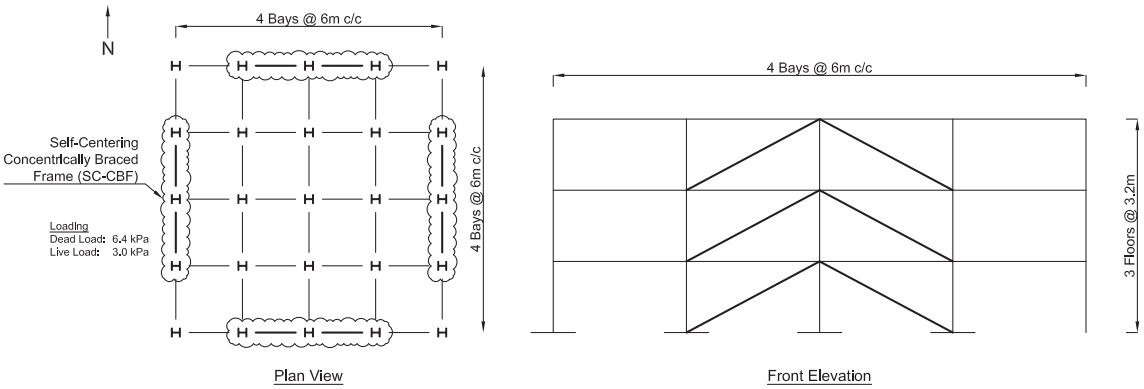

Figure 4.1. Layout of 3-storey SC-CBF**.**

4.2. Numerical Modelling

A numerical model was developed in OpenSees using the previously discussed connection details. A P-Delta column was also included to capture the second order effects during the analysis. Fibre-based elements using the force formulation were used for both beam and column with 5 fibres across the flange width and web depth, 2 fibres across the web and flange thicknesses and 3 integration points per element. The Guiffré-Menegotto Pinto (Steel02) hysteresis model was used to model the steel fibres with a yield strength of 355 N/mm^2 and a strain hardening ratio of 0.005. The braces were also modelled using fibre based elements with 20 fibres across the width and depth and 5 fibres across the thickness with 3 integration points per element, of which there are 2 per brace. The use of an initial camber in the braces to initiate brace buckling was developed by Uriz and Mahin (2008) and an initial camber of 0.5% was used as per more recent work by Salawdeh (2012). Also included was a fatigue model developed by Uriz and Mahin (2008) to simulate the effects of low cycle fatigue on the braces subjected to numerous inelastic cycles. The parameters for the fatigue model used are as per Salawdeh (2012) as these were calibrated for numerous quasi-static and shake table tests for tubular bracings.

4.3. Ground Motions

As previously mentioned, the ground motions used in this study correspond to the 10% in 50 year hazard level for the downtown Los Angeles area. The set of motions used here were developed to match spectral values as part of a SAC steel project and further reading can be found in Somerville *et al.* (1997). The set of motions consists of 10 records, of which there are two orthogonal components, giving 20 motions in total. These motions were further scaled by a factor of 0.9 to better match the design spectrum.

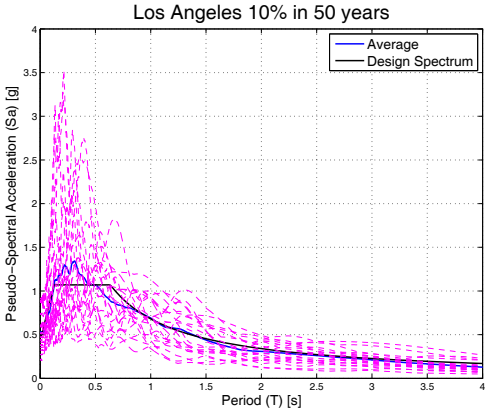

Figure 4.2. Design spectrum and corresponding ground motions.

4.4. NLTH Results and Discussion

In order to evaluate the performance of the SC-CBF subjected to the 20 ground motions, a number of parameters are used to investigate the performance of the system. Firstly, the code defined limits on interstorey drift must be satisfied, which are set at 2.5% for this structure. Other performance criteria are that the beams, column and PT elements must remain in the elastic range, and the brace members must also be within an acceptable ductility range.

Fig. 4.3 shows the interstorey drifts at each storey for all 20 ground motions, as well as the average values from the NLTH. It can be seen from this plot that the average of the response falls within the code defined limit for the SC-CBF. Another performance goal which is one of the principle objectives of using self-centering systems is to have minimal residual drifts. Clayton *et al.* (2012) defines a residual drift limit of 0.2% for a self-centering steel plate shear wall system under the same set of ground motions, as this corresponds to the out-of-plumbness limit for construction. Henry (2011) specifies a performance matrix for a self-centering concrete system, where for a DBE that corresponds to the DBE in this study, a limit of 0.2% was also specified. Eurocode 3 (EC3) (CEN, 2005) gives an expression in order to determine the acceptable out-of-plumbness tolerance for steel buildings. Using this expression for at the given building gives a limit of 0.272%, which is slightly larger than the limit used in other studies. In order to make this performance comparable, a residual drift limit of 0.2% was adopted here. In order to properly evaluate the residual drifts of the structure, the earthquake records were run for an additional 40 seconds of no excitation in order to let the system return to rest and properly evaluate the final position of the structure. Fig. 4.3 shows a plot of the residual drifts at each storey for all of the records and the corresponding average. This plot demonstrates the self-centering behaviour of the SC-CBF under the DBE where the average response is well below the prescribed maximum tolerance of 0.2%.

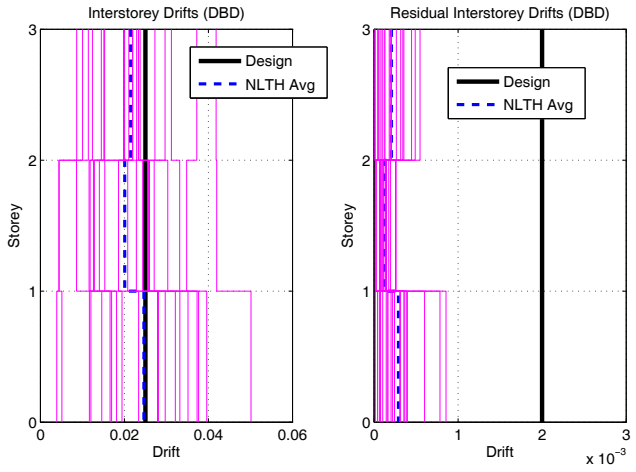

Figure 4.3. Interstorey drift and residual drifts.

In addition to the global performance of the system, the beams, columns and PT elements should remain elastic at all times. In order to evaluate this, the utilisation ratios (η) of the members at each level are plotted, where η_N, η_M and η_V represent the axial, flexural and shear utilisation ratios. To account for the interaction of axial and flexural capacity the sum of η_N and η_M should also be less than unity as per Eurocode 8 (CEN, 2004) requirement in Eqn. 4.2. Fig. 4.4 shows these utilisation ratios for the beams and columns where it can be seen that the ratios are all below unity, which satisfies the criteria that they remained elastic at all times during the response.

The other important requirement is that the PT elements remain elastic at all time during the response. Fig. 4.4 shows that the PT elements all remained elastic during the response. This is a critical requirement, as if the PT elements yield, the initial prestressing force will be lost and the self-centering

nature of the SC-CBF will be greatly reduced. Thus, these elements should be carefully detailed in order to avoid this. Another requirement is to avoid brace fracture during the response. Experimental investigation into the displacement ductility at which brace fracture occurs has been investigated (Goggins *et al.* 2005; Nip *et al.* 2010) and have shown that the fracture ductility to be a function of both the member ($\bar{\lambda}$) and cross section slenderness (e.g. width to thickness ratio), but many suggest that member slenderness is the most important parameter affecting facture ductility. On the other hand, an investigation into this by Huang and Mahin (2010) concluded that the increase in fracture ductility was more due to the width to thickness ratio and that the global slenderness had little influence on this. This may be due to stockier members being investigated by Huang and Mahin (2010). Through experimental and numerical investigation Nip *et al.* (2010) developed expressions for the fracture ductility of tubular braces, which were dependent on both the member and cross-sectional slenderness of the brace member. . These expressions are used in this current study to evaluate the performance of the braces to ensure that the ductility is not sufficient enough to cause brace fracture. It is also important to note that the braces were modelled to include the effects of low cycle fatigue, but none of the braces in the NLTH analyses experienced any fatiguing due to this effect. Fig. 4.4(d) shows a plot of the expected fracture ductility (μ_f) and the measured ductility demand (μ_D) for the braces used at each floor in the SC-CBF. From this it can be seen that the braces experienced ductility demands well below the fracture ductility level given by Nip et al. (2010) expressions for cold formed carbon steel.

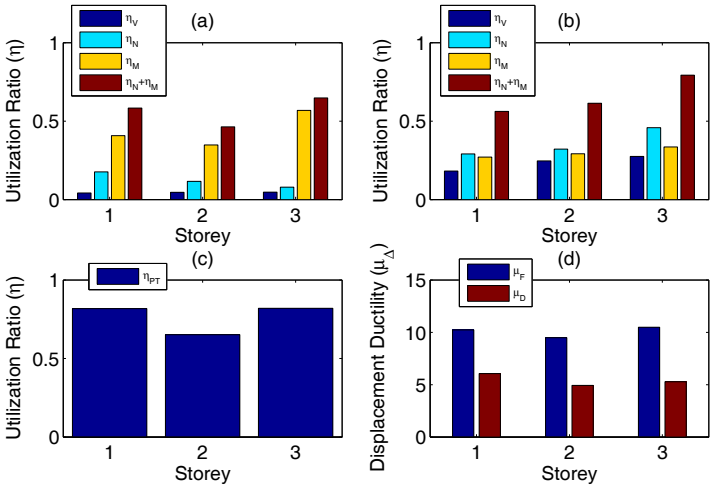

Figure 4.4. Utilisation ratios of the (a) beams, (b) columns, (c) PT elements and (d) brace ductilities.

5. CONCLUSIONS

The mechanics of a newly developed SC-CBF were presented in this paper. The general arrangement of the system was first discussed along with the derivation of expressions to describe the behaviour of the system. A numerical model developed in OpenSees was described along with an example frame, where the equations developed to describe the response were validated using this numerical model. A design example of a 3-storey SC-CBF was presented, where the frame was designed according to the force-based design procedure specified in Eurocode 8. This 3 storey SC-CBF was subjected to 20 ground motions that matched the design spectrum. The measured storey drifts for the SC-CBF satisfied code prescribed drift limits. Other specified performance levels were also satisfied, which included the requirement that the beams, columns and PT elements all remained elastic during seismic excitation. The ductility demands on the braces were examined to ensure the adequate ductile behaviour of the braces was achieved and that brace fracture was avoided. The system exhibited a self-centering nature, where the residual drifts were all well below the residual drift limit that correspond to standard construction tolerances, demonstrating the structure recentered following the analyses.

This study demonstrates that the SC-CBF presents a new and improved way to design and detail steel braced framing systems, when enhanced system performance is required. While the results presented here are promising in terms of design and performance, further work is required to validate the system and develop a more rigorous design procedure for a more complete performance based design framework. Accompanied by experimental testing, this will be the focus of future work.

ACKNOWLEDGEMENTS

The first author would like to gratefully acknowledge the funding provided by the Irish Research Council for Science, Engineering and Technology (IRCSET).

REFERENCES

Broderick B.M., Elghazouli A.Y. and Goggins J. (2008) Earthquake testing and response analysis of concentrically-braced sub-frames. *Journal of Constructional Steel Research*. **64:1**, 997-1007.

Comité Européen de Normalisation (CEN). (2004). Eurocode 8: Design of structures for earthquake resistance – part 1: General rules, seismic actions and rules for buildings. European Standard EN 1998-1:2004. Brussels, Belgium.

Comité Européen de Normalisation (CEN). (2005). Eurocode 3: Design of steel structures – part 1-1: General rules and rules for buildings. European Standard EN 1993-1-1:2005. Brussels, Belgium.

Christopoulos, C. (2002). *Self-Centering Post-Tensioned Energy Dissipating (PTED) Steel Frames for Seismic Regions*. PhD Thesis. University of California, San Diego, California, USA.

Clayton, P., Berman, J. and Lowes, L. (2012). Seismic design and performance of self-centering steel plate shear walls. *Journal of Structural Engineerin*g. **138:1**, 22-30.

English, J. and Goggins J. (2012). Nonlinear Seismic Response of Concentrically Braced Frames using Finite Element Models. *In Proceedings of 15th World Conference on Earthquake Engineering.* Lisbon, Portugal.

Garlock, M. (2002). *Design, Analysis, and Experimental Behaviour of Seismic Resistant Post-Tensioned Steel Moment Resisting Frames*. PhD thesis, Lehigh University, Lehigh, PA, USA.

Goggins, J., Broderick, B., Elghazouli, A. and Lucas, A. (2005). Experimental cyclic response of cold-formed hollow steel bracing members. *Engineering Structures*, **27:7**, 977-989.

Henry, R. (2011). *Self-Centering Precast Concrete Walls for Buildings in Regions with Low to High Seismicity*. PhD thesis. University of Auckland, New Zealand.

Huang, Y. and Mahin, S. (2010). Simulating the inelastic seismic behaviour of steel braced frames including the effects of low cycle fatigue. Technical Report 2010/104, Pacific Earthquake Engineering Research Center, California, USA.

McCormick, J., Aburano, H., Ikenaga, M. and Nakashima, M. (2008). Permissible residual deformation levels for building structures considering both safety and human elements. *In Proceedings of the 14th World Conference on Earthquake Engineering, Beijing, China.*

McKenna, F., Fenves, G., Filippou, F. and Mazzoni, S. (2000). *Open system for earthquake engineering simulation (OpenSees).* http://opensees.berkeley.edu/wiki/index.php/Main_Page.

Nip, K. H., Gardner, L. and Elghazouli, A. Y. (2010). Cyclic testing and numerical modelling of carbon steel and stainless steel tubular bracing members. *Engineering Structures,* **32:2**, 424-441.

Salawdeh, S. (2012). *Seismic Design of Concentrically Braced Steel Frames*. PhD thesis, National University of Ireland, Galway, Ireland.

Somerville, P., Smith, H., Puriyamurthala, S., and Sun, J. (1997). Development of ground motion time histories for Phase 2 of the FEMA/SAC steel project. Technical Report. SAC/BD 97/04 Prepared by the SAC Joint Venture for the Federal Emergency Management Agency, Washington, DC.

Uriz, P. and Mahin, S. (2008). *Towards earthquake resistant design of concentrically braced steel structures*. Technical Report 2008/08, Pacific Earthquake Engineering Research Center, California, USA.

Wijesundara, K. (2009). *Design of Concentrically Braced Steel Frames with RHS Shape Braces*. PhD thesis, European Centre for Training and Research in Earthquake Engineering (EUCENTRE), Pavia, Italy.